Available online at www.sciencedirect.com
SCIENCE DIRECT®
Biochemical Pharmacology 69 (2005) 781–790
Biochemical Pharmacology
www.elsevier.com/locate/biochempharm

Insulin-stimulated endothelial nitric oxide release is calcium independent and mediated via protein kinase B

Nicholas A. Hartell[a,*], Helen E. Archer[b], Clifford J. Bailey[b]

[a]*Department of Pharmacology, The School of Pharmacy, University of London, WC1N 1AX, UK*
[b]*School of Life and Health Sciences, Aston University, Birmingham, UK*

Received 14 August 2004; accepted 8 November 2004

Abstract

Insulin exerts a vasodilator effect by stimulating endothelial nitric oxide (NO) production. Studies in cultured cells suggest that insulin might activate endothelial nitric oxide synthase (eNOS) by an atypical, calcium-independent mechanism. This study investigates the mechanism of insulin-stimulated endothelial NO production in intact aortic wall. Real time fluorescence imaging with 4,5-diaminofluorescin diacetate (DAF-2 DA) or 4-amino-5-methylamino-2′,7′-difluorofluorescein diacetate (DAF-FM DA) and FURA 2-AM was used to simultaneously visualise NO and intracellular calcium concentrations at multiple locations in the endothelium and vascular smooth muscle of isolated rat and mouse aorta after exposure to insulin. Inhibitors of intracellular insulin signalling were used to determine the pathway for insulin-stimulated NO production. Unlike acetylcholine, which stimulated endothelial NO production with a typical increase in free intracellular calcium, insulin (10^{-8} to 10^{-6} M) stimulated endothelial NO production without elevating intracellular calcium levels. Insulin-stimulated NO production was concentration dependent and detected within 30 s of application. Peak increases in NO occurred between 60 and 120 s and declined slowly thereafter. Separate measurements of NO production by fluorescence of 2,3-diaminonaphthalene (DAN) noted that selective inhibitors of phosphatidylinositol 3-kinase (PI3K) and protein kinase B (PKB) inhibited insulin-stimulated NO production, whereas these inhibitors alone did not alter NO production or acetylcholine-stimulated NO production. Insulin-stimulated NO production by endothelium is an acute calcium-independent effect mediated via the PI3K-PKB signalling pathway.

Keywords: Insulin; Endothelium; Nitric oxide; Nitric oxide synthase; Calcium; Phosphatidylinositol 3-kinase; Protein kinase B

1. Introduction

Insulin exerts a direct vasodilator effect on the vascular wall [1]. This effect is mediated via the endothelium where insulin activates endothelial nitric oxide synthase (eNOS), catalysing the conversion of L-arginine to L-citrulline, and liberating nitric oxide (NO) [2–4]. NO passes into the sub-endothelial space and diffuses to the vascular smooth muscle (VSM). Within the VSM, NO binds to the haem group of guanylate cyclase, stimulating production of cyclic guanosine monophosphate. Raised cyclic guanosine monophosphate reduces the intracellular free calcium concentration, causing the VSM to relax [5,6].

The mechanism by which insulin activates eNOS is uncertain. Activation of eNOS is generally a calcium dependent process [7]. For example, the vasorelaxation effect of acetylcholine is mediated via muscarinic receptors that promote the release of calcium from intracellular stores. This raises the intracellular free calcium concentration, enabling calcium-calmodulin to bind to eNOS, displacing caveolin-1 and activating eNOS [8]. However, recent studies in cultured $3T3^{IR}$ fibroblasts expressing human insulin receptors and transfected with eNOS found that insulin rapidly activated eNOS without increasing intracellular free calcium [9]. Calcium-independent

Abbreviations: DAN, 2,3-diaminonaphthalene; DAF-2 DA, 4,5-diaminofluorescin diacetate; eNOS, endothelial nitric oxide synthase; IGF1, insulin-like growth factor-1; KRB, Krebs Ringer bicarbonate; L-NAME, *N*-nitro-L-arginine methyl ester hydrochloride; MAP, mitogen-activated protein; NO, nitric oxide; PI3K, phosphatidylinositol 3-kinase; PKB (Akt), protein kinase B; ROI, region of interest; VSM, vascular smooth muscle

* Corresponding author. Tel.: +44 207 753 5897; fax: +44 207 753 5902.
E-mail address: nicholas.hartell@ulsop.ac.uk (N.A. Hartell).

0006-2952/$ – see front matter © 2004 Elsevier Inc. All rights reserved.
doi:10.1016/j.bcp.2004.11.022

activation of eNOS is not unknown since there have been reports that insulin-like growth factor-1 (IGF1), oestrogens and shear stress can increase NO production by endothelium without increasing intracellular free calcium [10–12]. Such a mechanism of activation of eNOS might involve protein kinase B (PKB (Akt)), which has recently been shown to phosphorylate eNOS and alter its sensitivity to calcium so that it is active at sub-physiological concentrations [9,13,14]. PKB is a post-receptor insulin signalling intermediate for stimulation of glucose transport [15].

Herein, we examine the effect of insulin on rat and mouse arterial wall using digital fluorescence imaging with simultaneous real time measurements of intracellular calcium and NO at multiple sites in the endothelium and VSM. Additionally, we have measured insulin-stimulated NO production with inhibitors of the insulin signalling cascade to identify the intracellular pathway involved.

2. Materials and methods

2.1. Chemicals

Chemicals and their sources were: 2,3-diaminonaphthalene (DAN) from Sigma, Poole, UK; 4,5-diaminofluorescin diacetate (DAF-2 DA) and wortmannin from Calbiochem, Nottingham, UK; 4-amino-5-methylamino-2′,7′-difluorofluorescein diacetate (DAF-FM DA) from Molecular Probes; SB202190 (p38 MAP kinase inhibitor) and hydroxymethyl-chiroinositol-methyl-octadecyl-carbonate (PKB inhibitor) from Merck Biosciences. Other chemicals were from Sigma–Aldrich, VWR International and Fisher Scientific. Plastic ware was from Sarstedt.

2.2. Tissue preparation

Slices and small segments of aorta were prepared from 16 to 20-week-old, homozygous normal lean (+/+) mice of the Aston colony or from weanling, male, Wistar rats. The animals were maintained as described elsewhere [16]. Mice were killed by cervical dislocation and rats were anaesthetised with isofluorane and decapitated. In both species, the thoracic aorta was carefully removed, rinsed in ice cold, modified Krebs Ringer bicarbonate (KRB) buffer [17] at room temperature and connective tissue carefully removed. Approximately, 1 cm sections were cut in half longitudinally to expose the luminal surface. The outer (adventitious) surface of the aorta was placed onto a nitrocellulose membrane (13 mm diameter, 0.45 μm pore size; Millipore Corporation), which was secured to a marble stage at its edges with small amounts of silicon grease. Slices approximately 0.5 mm thick were cut with a Machilwain tissue slicer.

2.3. Preliminary spectrofluorimetric nitric oxide assay

Five milligrams segments of aorta were cut from slices with butterfly scissors and placed one per well in a 96 well plate. Each well contained 100 μl KRB buffer at 22 °C pregassed with 95% O_2:5% CO_2. The buffer was supplemented with 10 μmol DAF-2 DA dye for 30 min, and then washed twice with KRB buffer to remove free (extracellular) dye. Tissue was incubated in KRB at 22 °C and NO production was measured at intervals for up to 1 h until there was a stable basal level. NO production was measured using a microplate spectrofluorimeter (Gemini Spectromax XS, Molecular Devices Corporation) with Softmaxpro software. The dye was excited at 490 nm and the emission was detected at 515 nm. Insulin (10^{-8} or 10^{-6} M) was added to the incubation medium and NO production was measured at 1 min intervals for 6 min. The principle of this NO assay relies on the DAF-2 DA dye readily permeating cells where it is hydrolysed by intracellular esterases to generate DAF-2 [18]. This active form of the dye fluoresces on interaction with NO.

2.4. Simultaneous imaging of nitric oxide and calcium

Slices of aorta on nitrocellulose membranes were fixed between parallel tracks of silicon grease on the bottom of a perfusion chamber. Slices were either placed on their side to examine the endothelium and VSM in cross-section (transverse orientation) or with the endothelial cells uppermost (luminal orientation). The tissue was immersed in 1 ml of gassed KRB buffer containing 10 μmol DAF-2 DA or 10 μmol DAF-FM DA and 10 μmol FURA-2AM and incubated at room temperature for 30 min. Compared to DAF-2, DAF-FM is reported to be more photostable, relatively insensitive to changes in pH above pH 5.5 and have a greater sensitivity to NO [19]. Thereafter, the tissue was washed for at least 30 min with KRB buffer before being transferred to the microscope where it was superfused with KRB buffer at 2 ml/min at room temperature. After a further equilibration period of at least 10 min to assess baseline rates of fluorescence changes, test substances (acetylcholine or insulin) were added to the perfusion buffer at the concentrations and for the durations.

Simultaneous measurements of calcium and NO were obtained by alternating excitation wavelengths of 350, 380, and 490 nm with a monochromator (Polychrome II; Till Photonics) over a 6 s period. Emitted light (515–545 nm) was collected with a charge-coupled device camera (C4880-81, Hamamatsu) attached to an upright microscope (BX50 WI, Olympus). The monochromator and camera were controlled with Openlab Software (Improvision). Data were processed offline with Igor Pro Software (Wavemetrics Inc.) using custom procedures. Free cytosolic calcium concentrations were estimated from ratio images created online from images collected at 350 and 380 nm using established methods [20]. Regions of interest

(ROI) were identified and average changes in fluorescence intensity for each ROI were calculated over time. In luminal orientation regions, encompassing individual endothelial cells were distinguished from those encompassing areas of smooth muscle by their characteristic response to brief applications of acetylcholine. Data from up to 15 separate endothelial or smooth muscle regions were pooled per slice. These ROIs were then transferred to images collected at 490 nm and used to measure simultaneous changes in DAF fluorescence. The same approach was used for transverse slices although it was not possible to distinguish individual cells in this orientation. Unlike Fura-2, DAF is not a ratiometric dye. Therefore, changes in fluorescence (ΔF) were normalised to the initial baseline fluorescence intensity (F_0) for each region. Since it is the rate of change of DAF fluorescence that is proportional to NO concentration [21], in some cases, the rate of change of fluorescence over unit time was calculated. Images illustrating changes in calcium or DAF fluorescence over time were also generated using the same procedures. To identify acetylcholine responsive cells, changes in calcium levels above a threshold value were superimposed upon background images of DAF fluorescence. Images illustrating changes in DAF fluorescence with respect to baseline levels were constructed by subtracting images collected at identified times from a baseline (ΔF). The data illustrated represent typical results obtained during more than three replicates of each procedure.

The specificity of DAF-2 as a NO sensor and its susceptibility to photoactivation has been reviewed recently [22]. Our data underwent a persistent and gradual increase in fluorescence with DAF-2, but this was less evident with DAF-FM. Since images were acquired at constant intervals it was possible to separate the effects of applications of acetylcholine or insulin from any non-specific effects, including photoactivation, by extrapolating baseline rates of changes in fluorescence and subtracting these from the data. The data presented therefore represent drug-induced changes in DAF-2/DAF-FM fluorescence with respect to normalised baseline levels. Consequently, no attempt to make a quantitative comparison between different experiments has been made. However, because the effects of acetylcholine on calcium mobilisation were routinely tested to allow us to assess the viability of the preparation and to distinguish endothelial cells from VSM, we were able to compare the relative changes in NO and calcium production within different regions of the same piece of tissue.

DAF-2 has also been reported to be sensitive to changes in calcium and magnesium [22] and able to react with dehydroascorbic acid and ascorbic acid, which often colocalise with NOS, causing an attenuation of NO-dependent signals [23]. The reported sensitivity of DAF-2 to calcium and magnesium [22] has recently been disputed by the makers of the dye who found that this was an indirect consequence of the calcium sensitivity of NO generating systems [24]. In our experiments, we found no qualitative difference between results obtained with DAF-2 and DAF-FM, which is reported to have fewer non-specific effects [19]. Our simultaneous measurements of both forms of DAF and calcium revealed that the two signals were capable of independent change and so we can be reasonably sure that changes in calcium did not directly influence DAF-2/DAF-FM fluorescence. Moreover, since our principal observation is that insulin increases DAF-2/DAF-FM fluorescence without a concurrent increase in calcium, any potential influence of calcium on DAF-2/DAF-FM fluorescence has no impact on our conclusions. We can also be confident that our measurements with DAF-2 and DAF-FM do not reflect significant changes in other reactive oxygen species since they were sensitive to LNARG and because DAF-2 has been shown to distinguish between NO and reactive oxygen species [25].

2.5. Nitrite assay for nitric oxide

Five milligrams segments of mouse aorta with an intact endothelium were placed one per well in a 96 well plate. Tissue was incubated for 30 min at 22 °C in 200 μl calcium-free KRB, since calcium can interfere with the method of NO measurement used in this experiment. Tissue was incubated with or without test substances (specific inhibitors of insulin signalling or eNOS) for 30 min followed by insulin (10^{-6} M) for 10 min. The tissue was then removed, digested in 2.8 M NaOH, and protein was determined by the bicinchoninic acid method [26]. Medium remaining in each well was assayed for nitrite by a fluorometric method in which nitrite is reacted with DAN to form the fluorescent product 1-(H)-naphthotriazole [27]. Briefly 50 μl DAN (0.05 mg/ml in 0.62 M HCl) was added to each well at room temperature for10 - min, and the reaction was terminated with 10 μl of 2.8 M NaOH. Fluorescence was read with excitation and emission wavelengths of 365 and 450 nm, respectively, using a Gemini Spectromax XS fluorimeter (Molecular Devices Corporation, Sunnyvale, CA, USA). Quantification was made against a standard curve of $NaNO_2$ in incubation buffer, and the accuracy and sensitivity were as previously defined [27]. Data are expressed as nitrite concentration (μM) per 100 μg protein.

2.6. Statistical analyses

For the reasons outlined above, statistical comparisons between imaging data from different aortic slices were not made. Comparisons were made between changes in DAF-2/DAF-FM and Fura-2 fluorescence levels between endothelial cells and VSM in the same slice. All such data are representative of at least five experiments. Other data are expressed as mean ± S.E.M. and compared by analysis of variance (ANOVA) with a post-hoc Dunnett's test or Student's unpaired *t*-test with a Bonferroni correction.

Probability differences of $p < 0.05$ were accepted as significant.

3. Results

3.1. Insulin-stimulated NO production in rat and mouse aorta

Suitability of rat and mouse aorta as a model to study the time- and concentration-dependency of insulin-stimulated NO production was established by preliminary static incubation experiments with small aortic segments. Data from mouse aorta are shown as an example in Fig. 1. Accurate quantitative fluorometric determination of NO production using DAF-2 fluorescent dye noted that in mouse aorta insulin (10^{-8} and 10^{-6} M) increased NO production (by approximately 20 and 35%, respectively) within 1 min (Fig. 1A). Similar increases in NO production were produced with acetylcholine (10^{-8} and 10^{-6} M) (Fig. 1B).

3.2. Simultaneous calcium and NO measurement in aortic slices

To investigate the acute time-dependency and calcium involvement of NO production in the endothelium, and to distinguish the endothelium from the VSM in an intact slice of aorta, simultaneous, real time, fluorescence imaging of NO and calcium was undertaken in slices of rat aorta in both transverse and luminal orientations. As already discussed, DAF-2 in particular is susceptible to photoactivation, leading to a steady increase in fluorescence over time. Therefore, in all experiments, a period of at least 5–10 min was allowed, prior to drug application, to allow an accurate assessment of baseline fluorescence levels. Once steady baseline levels of DAF-2/DAF-FM fluorescence and calcium levels were established, acetylcholine (1 or 10 μM) was superfused for a period of 1 min. Individual, more brightly fluorescent cells could be identified on the luminal surface of slices incubated with DAF-2 or DAF-FM (see Fig. 2A). Superfusion with acetylcholine immediately increased the calcium levels in most of these cells on the luminal surface (Fig. 2A and C). Those cells that did respond were identified as healthy endothelial cells. Despite the relatively slow sampling rate, two clear phases of calcium mobilisation could be seen. An initial fast peak, indicative of calcium release from inositol-1,3-bis-phosphate sensitive intracellular stores was followed by a slower, prolonged response that is due to calcium influx for a review see [28]. Non-responsive, inter-endothelial regions were collectively identified as being VSM. After a short delay of between 30 and 70 s, a steady increase in DAF-2/DAF-FM fluorescence was observed in all regions (Fig. 2B and C). Since it is the rate of change of DAF fluorescence that is proportional to NO concentration [21], the change in DAF-2/DAF-FM fluorescence was differentiated to yield the instantaneous slope ($\Delta F/\Delta t$). In this orientation, little if any difference in the absolute amount or rate of DAF fluorescence increase was observed between identified endothelial or smooth muscle regions (Fig. 2C).

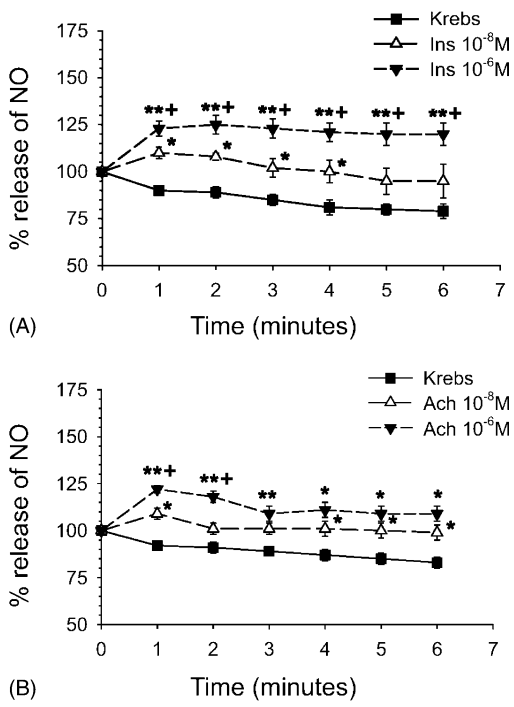

Fig. 1. The effects of (A) insulin (10^{-8} and 10^{-6} M) and (B) acetylcholine (10^{-8} and 10^{-6} M) on NO release from incubated segments of mouse aorta. NO was measured by DAF-2 fluorescence. NO is shown as the percentage change from baseline at time zero, mean ± S.E.M., $n = 6$. Treatment effects were significantly different from control ($p < 0.01$) by ANOVA, and mean values at individual time points were significantly different between treatments and control ($^{*}p < 0.05$ and $^{**}p < 0.01$), and between different concentrations of test substance ($^{+}p < 0.05$) by Dunnett's test.

Experiments were repeated in rat aortic slices placed on their side (transverse orientation) to allow measurement of fluorescence in widely separate layers of the aortic slices. In this orientation, acetylcholine caused a similarly large increase in calcium that was restricted to the luminal surface of slices (Fig. 3A and C). The apparent, small increase in calcium in the VSM in this example, where the increase in endothelial calcium was substantial, was almost certainly due to light reflecting from endothelial regions. This spillover effect was much reduced in cases where the calcium increase was less substantial (see for example Fig. 6). Moreover, acetylcholine had no effect on VSM in tissue that was stripped of its endothelial layer (data not shown). As with slices placed with the luminal surface uppermost, increases in DAF-FM fluorescence were observed several tens of seconds after the initial increase in calcium (Fig. 3B and D). In this example, a delayed increase in DAF-2 fluorescence was observed in the VSM 10–15 s later. The extent of spread of the NO signal to the VSM was very variable between tissues and dependent on the responsiveness of individual slices. In cases where the increase in DAF-2/DAF-FM fluorescence was compara-

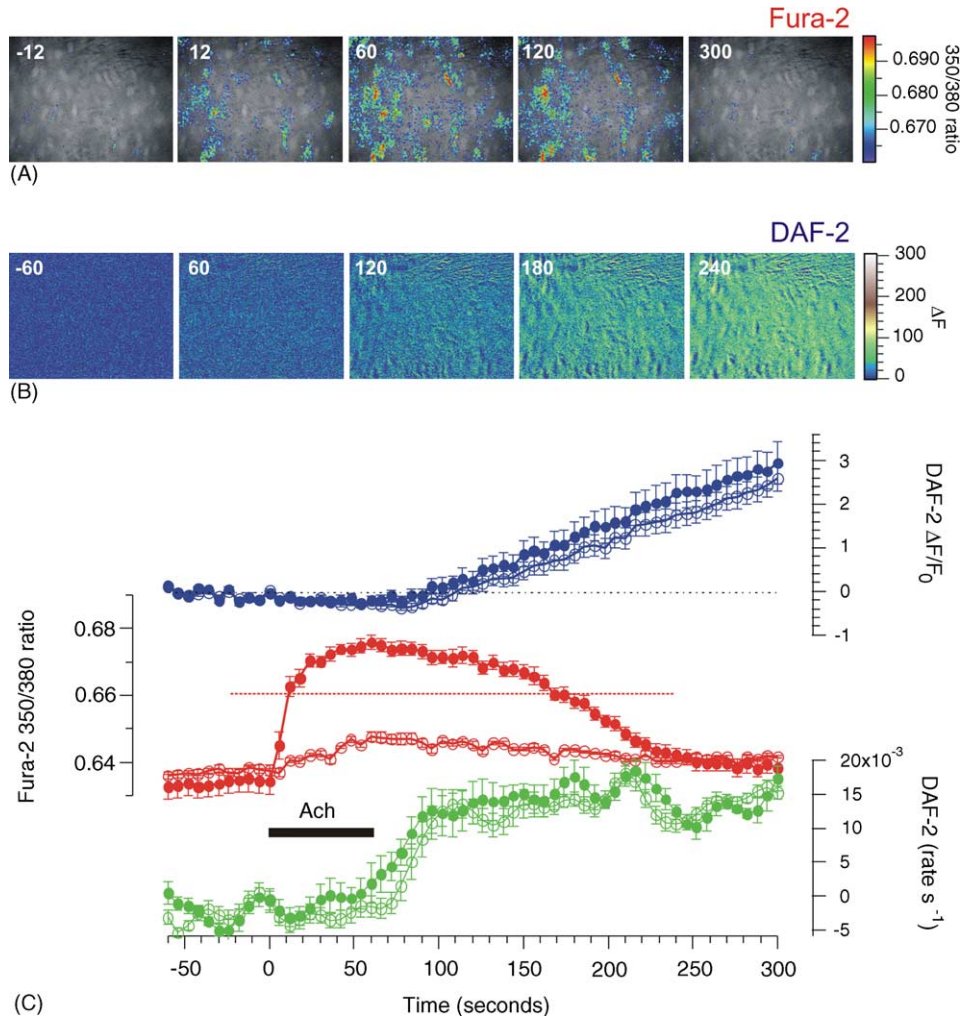

Fig. 2. NO levels rise after acetylcholine induced increases in intracellular calcium in endothelial cells. (A) representative example of a rat aortic slice positioned with the luminal side uppermost loaded with the NO indicator DAF-2 DA and the calcium indicator Fura-2 AM (10 μM each applied externally). The times on each image represent the times in seconds at which the images were taken. The intensities of ratio images (350/380 nm) above an arbitrary threshold value of 0.66 were pseudocoloured and shown superimposed upon a greyscale background image of DAF-2 fluorescence, captured using an excitation wavelength of 490 nm. Note that individual endothelial cells can be identified on the background image. (B) Pseudocoloured changes in DAF-2 fluorescence with respect to an image captured at time zero are shown. The times on each image represent the times in seconds at which the images were taken and correspond to the blue circles in panel C. (C) Changes in DAF fluorescence (ΔF) normalised to mean baseline values (F_0) are shown ($\Delta F/F_0$), along with simultaneous measurements of Fura-2350/380 ratio images (red traces). Shown below is the rate of change of DAF-2 fluorescence (green). The filled circles in each graph represent ROIs placed over endothelial cells and the open circles represent VSM. Individual data points represent the means and standard errors of 10 endothelial regions and 8 VSM regions. The horizontal red dotted line shows the threshold level used to generate the images in (A).

tively small, little or no spread of the NO signal beyond the endothelial layer was observed (compare Figs. 3D and 6A). NO-dependent relaxation of VSM in intact preparations is far more rapid than the observed increases in DAF-2/DAF-FM fluorescence. The consistent delay between the endothelial calcium elevation and the increase in DAF-2/DAF-FM fluorescence, and any additional delay for the signal to appear in the VSM, presumably reflects, therefore, the time taken for NO to accumulate to concentrations approaching the threshold detection limits of 3–5 nM of the dyes [19,29]. That these experiments were carried out at room temperature (21–23 °C) may have also contributed to delay.

These results are entirely consistent with the established notion that acetylcholine elevates intracellular calcium in endothelial cells and this triggers NOS activation and production of NO, which then diffuses to the underlying VSM. To confirm this, acetylcholine was applied in the presence of the NOS inhibitor L-NAME (10 μM) and then again in the same tissues after its thorough washout. As shown in Fig. 4, the actions of acetylcholine on DAF-2 fluorescence were significantly attenuated when NOS activity was reduced.

3.3. Insulin effects on calcium and NO in aortic endothelium and VSM

Having established that these two imaging techniques can be used to assess NO and calcium signalling in endothelial and VSM regions of rat aortic slices, we next

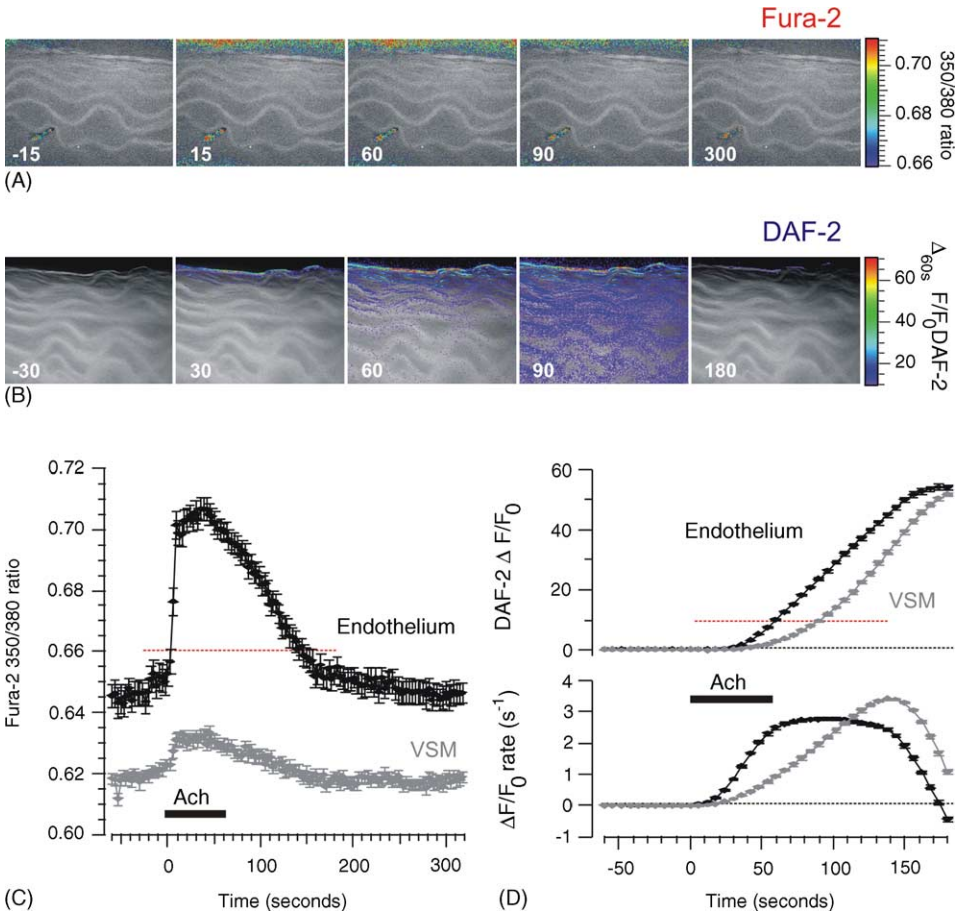

Fig. 3. Selective increase in NO in endothelial layers of aortic slices after acetylcholine induced increases in intracellular calcium in endothelial cells. (A) representative example of a rat aortic slice positioned on its side with the luminal side at the top of the image, loaded with Fura-2 AM (10 μM). The intensities of ratio images (350/380 nm) above a threshold value of 0.69 were pseudocoloured and shown superimposed upon a greyscale background image captured before acetylcholine application. In this example and in the example shown in panel B, the endothelial layer extends backwards, at an angle, below the plane of focus and so it looks thicker than a single cell layer. Note also the presence of elastic fibres running through the VSM. (B) In a separate slice loaded with DAF-FM DA (10 μM), changes in DAF-FM fluorescence before and after application of acetylcholine are shown. The differences in fluorescence between pairs of images captured at 60 s intervals were calculated at different time points and the resulting difference image was divided by the first of the pair ($\Delta_{60s}F/F_0$). Images were then thresholded and values above 10 were psuedocoloured and superimposed on a greyscale background image. (C) Changes in Fura-2 ratio values following application of acetylcholine are shown for endothelial (black trace) and VSM regions (grey trace) from the same slice shown in panel A. (D) DAF fluorescence (ΔF) normalised to mean baseline values (F_0) shown ($\Delta F/F_0$) for the slice illustrated in panel B. measurements from regions of interest placed over endothelial regions are shown in black and those from VSM are shown in grey. Individual data points represent the means and standard errors of seven endothelial regions and seven VSM regions. The horizontal red dotted lines in (C and D) illustrate the threshold levels used to generate the images in (A and B), respectively. Shown underneath are the differentials of the data illustrating the rate of fluorescence change over unit time.

examined the effects of insulin on these two second messengers in this preparation. Superfusion of rat aortic slices with insulin produced substantial increases in NO in both endothelial and VSM layers that were comparable to those produced by acetylcholine (Fig. 5). Insulin-stimulated NO production was concentration dependent and responses were detected at concentrations as low as 10 nM (Fig. 5B). Increases in DAF-2/DAF-FM fluorescence were detected within 30 s. The peak rate of fluorescence increase, which corresponds to the time when NO production is maximal [21], occurred between 60 and 120 s of insulin application. The relative potency of insulin was compared to that of acetylcholine by measuring rates of DAF-2 fluorescence increase over a 1 min period during applications in the same slice (Fig. 5A). Concentrations of insulin between 1 and 10 μM produced responses that were similar to those produced by 10 μM acetylcholine. Near maximal increases in NO were produced by prolonged applications of 10^{-8} M insulin, and only small further increments were observed with additional insulin up to 10^{-6} M (Fig. 5B). Importantly, the intracellular calcium levels measured by FURA 2 in both endothelium and VSM were unchanged by any of the insulin concentrations tested, despite the prompt rise in NO.

3.4. PKB and PI3K mediate insulin-induced NO production

We next set out to identify the signalling pathway responsible for this insulin-mediated, calcium-independent increase in NO production. Insulin promotes NO production from endothelial cells via the phosphatidylinositol-3-

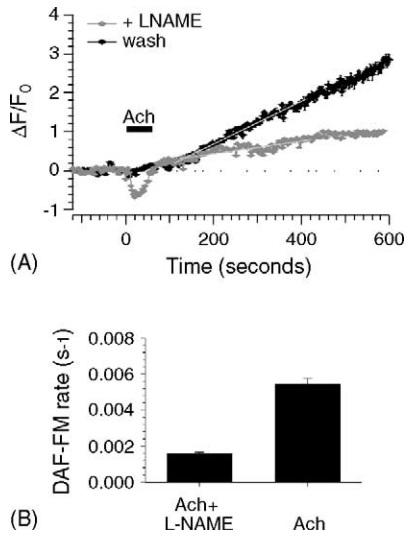

Fig. 4. Inhibition of NOS reduces acetylcholine induced increases in DAF-FM fluorescence. (A) Mean ± S.E.M. changes in DAF fluorescence from 15 identified endothelial cells on the luminal surface of a rat aortic slice are shown. Acetylcholine was applied for 1 min in the presence of L-NAME (grey trace) and then again after washing for 30 min (black trace). (B) Mean ± S.E.M. rates of fluorescence increase from these regions following acetylcholine application are illustrated in the presence and absence of L-NAME.

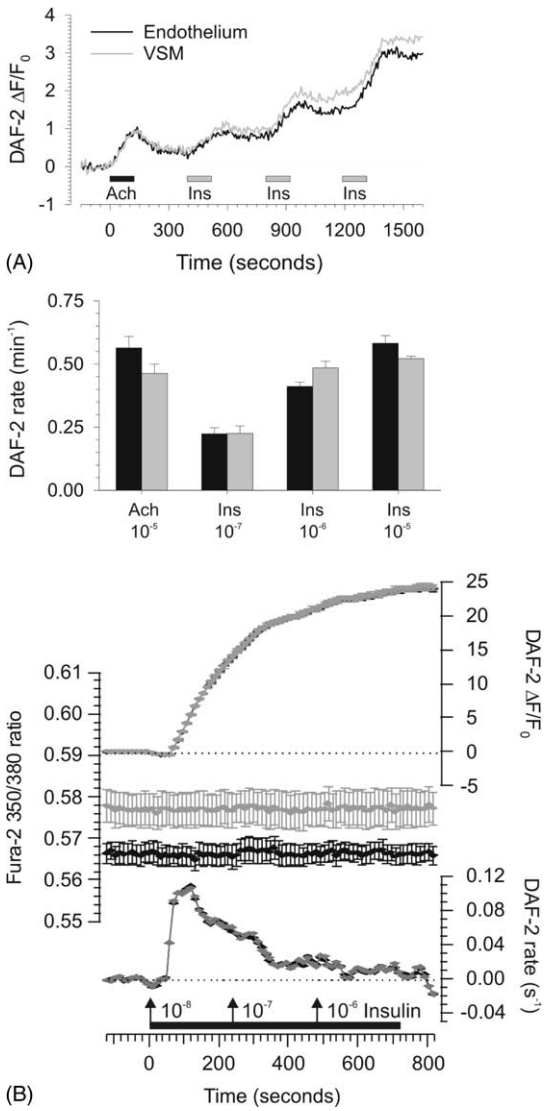

Fig. 5. Brief applications of insulin induce concentration dependent increases in DAF-2 fluorescence without concurrent increases in intracellular calcium in either endothelium or VSM. (A) A 2 min application of acetylcholine (Ach; 1 μM) was followed by applications of insulin (Ins; 0.1, 1 and 10 μM) to a rat aortic slice. Mean fluorescence changes relative to baseline levels are shown for nine endothelial (black trace) and eight VSM regions (grey trace). The mean ± S.E.M. peak rates of fluorescence change for endothelial and VSM regions were measured over a 1 min period during each application and are shown below. (B) Insulin was applied in a cumulative manner to aortic slices incubated with DAF-2 DA and Fura-2 AM. Insulin elevated DAF-2 fluorescence at a concentration of 10 nM. Subsequent applications at higher concentrations had no additional effect. No increase in Fura-2 fluorescence was observed over this entire concentration range. Endothelial regions are depicted in black and VSM in grey.

kinase (PI3K) pathway [30], which is an upstream regulator of PKB. Phosphorylation of endothelial NOS by PKB has been reported to lower the calcium sensitivity of eNOS, causing it to become active at sub-physiological concentrations of calcium [13,14]. We therefore compared the effects of the selective PI3K inhibitor wortmannin [13,31] on acetylcholine (calcium dependent) and insulin (calcium-independent) mediated NO production. Incubation of rat aortic slices with wortmannin (10 μM) for 30 min had no effect on the ability of acetylcholine to elevate either calcium in endothelial cells or to trigger NO production (Fig. 6A and B). In contrast, wortmannin reduced insulin dependent increases in NO production (Fig. 6B and C).

To further confirm the identity of the signalling pathway through which insulin stimulates NO release, nitrite determinations were made as an index of NO production during incubation experiments with segments of aorta. In the example illustrated in Fig. 7, mouse aortic slices were incubated with insulin (10^{-6} M) for 10 min. This increased NO production by almost 500%, compared with a 400% increase with acetylcholine (10^{-6} M) (Fig. 7). When the tissue was incubated with wortmannin (5 nM) and the structurally unrelated PI3K inhibitor LY294002 (1.4 nM) before exposure to insulin, insulin-stimulated NO production was substantially reduced. Insulin-stimulated NO production was also reduced by prior incubation with the PKB inhibitor, hydroxymethyl-chiroinositol-methyl-octadecylcarbonate (5 μM) [32], but not by prior incubation with the p38 MAP kinase inhibitor, SB202190 (16 nM). None of these inhibitors altered basal NO production alone or when stimulated with acetylcholine (data not shown).

4. Discussion

The ability of insulin to stimulate nitric oxide synthase and increase NO production is well established [1]. However, much of the evidence derives from cultured cells,

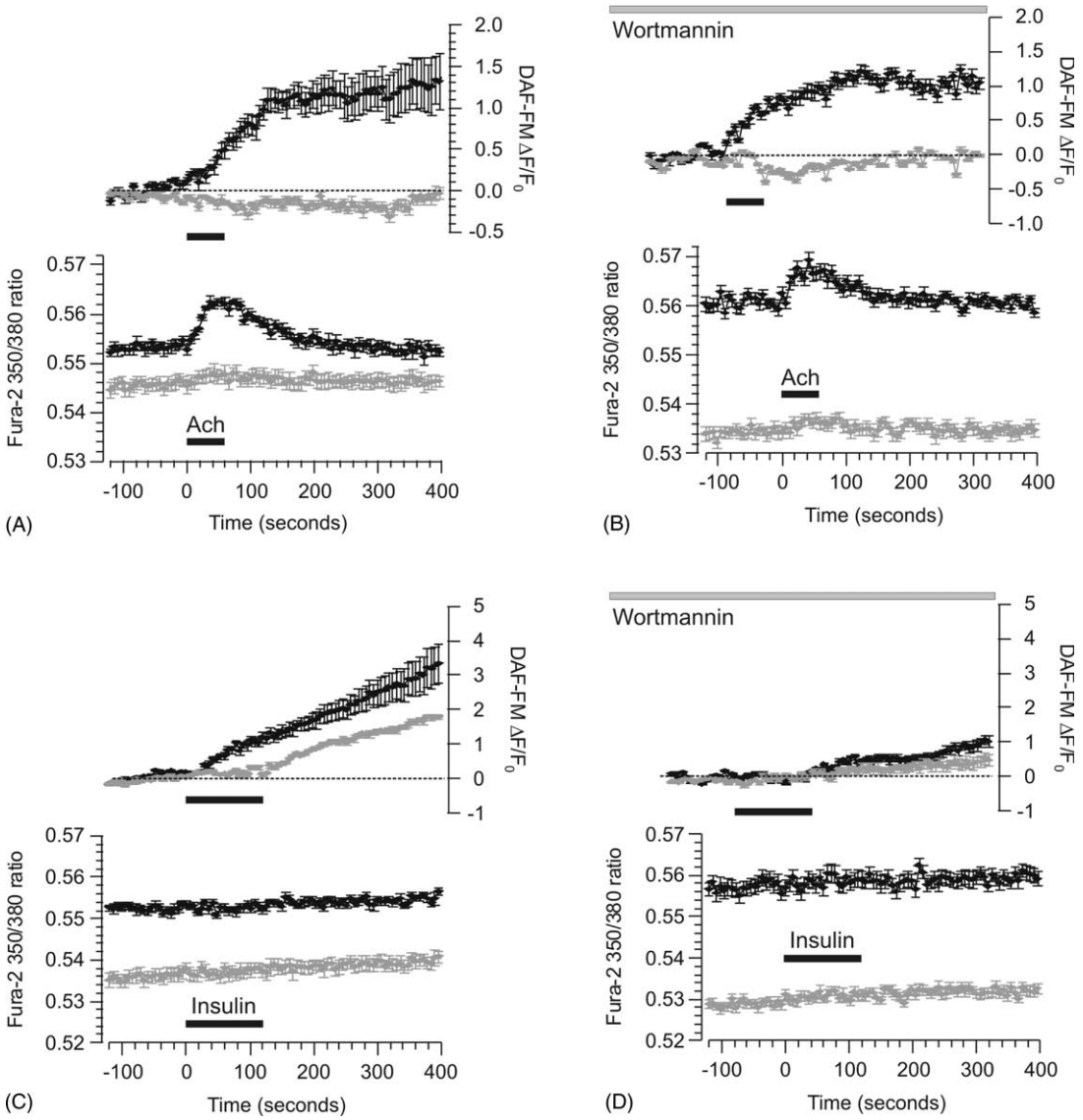

Fig. 6. The effects of wortmannin on acetylcholine and insulin-dependent NO production. (A) Acetylcholine was applied to transverse rat aortic slices incubated with Fura-2 AM and DAF-FM DA. The mean ± S.E.M. of six endothelial (black symbols) and six VSM regions (grey symbols) are shown. (B) Illustrates the actions of a second application of acetylcholine (1 μM) in the presence of 1 μM wortmannin. The effects of applications of 1 μM insulin are shown in the absence (C) and presence (D) of wortmannin. All experiments were carried out in the same slice. Experiments shown in panels A and C preceded those in B and D.

often not endothelial cells or cells transfected to over-express insulin receptors or eNOS, and the mechanism by which insulin stimulates eNOS in normal intact endothelium has not been fully resolved [9,33]. Herein, the use of real time simultaneous fluorescence imaging for NO and intracellular calcium in intact aortic wall has demonstrated that insulin-stimulated NO production by the endothelium is different to that of acetylcholine: the effect of insulin is independent of calcium and mediated by the PI3K-PKB intracellular signalling pathway.

Real time, simultaneous measurements of NO and intracellular calcium in the present superfusion system have demonstrated that insulin-stimulated NO production can be rapid in the intact endothelium of mouse and rat aorta, reaching a maximum within 60–120 s, compared with a slower peak at 1–2 min or longer in most cultured isolated cells [9,30,33–35]. The present studies were conducted at room temperature to discriminate the relative time-dependent effects on calcium and NO. The effects are too rapid at 37 °C (data not shown) to allow temporal discrimination of the component effects. The mouse and rat aorta data are consistent with recent evidence from fibroblasts transfected with eNOS in which insulin continued to stimulate NO production in the presence of a calcium chelator, indicating a calcium independent mechanism [9]. Stimulation of eNOS by PKB is known to be independent of calcium and involve phosphorylation of a serine residue (S1179 for bovine eNOS) [9,14,34]. Indeed, a point mutation at this residue (S1179A) prevents stimulation of eNOS by PKB [9]. Overexpression of

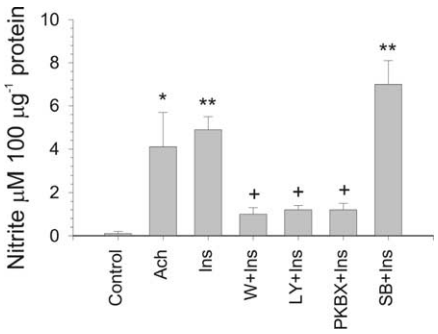

Fig. 7. Effect of acetylcholine, insulin, inhibitors of insulin signalling (the PI3K inhibitors wortmannin and LY294002; the PKB inhibitor hydroxymethyl-chiroinositol-methyl-octadecylcarbonate, and the MAP kinase inhibitor SB202190) on NO release by incubated segments of mouse aorta. NO was measured by DAN fluorescence and expressed as nitrite concentration. Values are mean ± S.E.M., $n = 6$. $^{*}p < 0.05$, $^{**}p < 0.01$ vs. control; $^{+}p < 0.05$ vs. insulin alone by Student's unpaired *t*-test.

insulin receptors increases insulin-stimulated NO production while an ihibitory mutation of IRS-1 or inhibition of PI3K has been shown to prevent the NO-increasing effect of insulin [34,36]. Linking these pieces of information, the present observations in the intact endothelium provide a compatible explanation that the calcium-independent stimulation of eNOS by insulin is mediated through the IRS-1—PI3K-PKB signalling pathway. Since the MAP kinase inhibitor SB202190 did not reduce insulin-stimulated NO release, it is likely that this intracellular pathway of insulin action is not required for insulin to acutely activate eNOS.

The calcium-independent stimulation of eNOS by insulin is consistent with an early report that IGF1 can rapidly raise NO production by cultured endothelial cells independently of any rise in the intracellular free ionised calcium concentration [12]. This could potentially involve either receptor cross-talk or signalling interaction of the IGF1 receptors with post-receptor components of the PI3K-PKB pathway as seen with the insulin-like effect of IGF1 on glucose uptake [15]. Some other rapidly acting calcium-independent activators of eNOS have been identified, notably oestadiol and fluid shear stress [10–12] and recent studies suggest that these might stimulate eNOS by phosphorylation through the PI3K-PKB pathway [37]. Indeed insulin may increase responsiveness to the calcium-independent activation of eNOS by oestradiol and fluid shear stress [10,37]

Although the vasodilator effect of insulin is weak, and in isolation this would appear to have only a minor physiological role, it may be more important when considered in the context of the metabolic effects of insulin [6,38]. Use of the same intracellular signalling pathway for insulin to acutely increase both NO release and translocation of glucose transporters into the cell membrane suggests a coordinated physiological process for insulin to facilitate increased perfusion and increased glucose transport in tissues such as skeletal muscle [6,33,38,39]. Moreover, use of the same signalling pathway for these physiological actions lends support to the concern that insulin resistance has diverse implications for metabolic and cardiovascular events, potentially sharing similarities of aetiology and pathogenesis [4,6]. Indeed there is now evidence that mice with IRS-1 knockout or an inhibitory mutation of PI3K develop hypertension as well as resistance to the metabolic effects of insulin [34,40]. Also the signalling pathway through the insulin receptor, IRS-1, PI3K and PKB is impaired in the vasculature of obese, glucose intolerant and insulin resistant fa/fa rats [40] and vascular function is impaired in mice with a 95% knockout of insulin receptors in endothelial cells [41]. Additionally, acute vasodilator responses involving NO production are impaired in human insulin resistance and diabetic states, and improved by insulin therapy [4,6,38,42,43]. Hence, a treatment strategy to rectify defects in the signalling pathway through PKB should benefit both metabolic and vascular aspects of insulin resistance.

In conclusion, the present study has provided real time visualised evidence in the intact vascular wall that insulin can acutely stimulate NO production by a calcium-independent mechanism that requires integrity of the PI3K-PKB signalling pathway.

Acknowledgements

This work was funded in part by grants from the Royal Society and BBSRC (NAH).

References

[1] Hsueh WA, Law RE. Insulin signaling in the arterial wall. Am J Cardiol 1999;84:21J–4J.
[2] Scherrer U, Randin D, Vollenweider P, Vollenweider L, Nicod P. Nitric oxide release accounts for insulin's vascular effects in humans. J Clin Invest 1994;94:2511–5.
[3] Steinberg HO, Brechtel G, Johnson A, Fineberg N, Baron AD. Insulin-mediated skeletal muscle vasodilation is nitric oxide dependent. A novel action of insulin to increase nitric oxide release. J Clin Invest 1994;94:1172–9.
[4] Petrie JR, Ueda S, Webb DJ, Elliott HL, Connell JM. Endothelial nitric oxide production and insulin sensitivity. A physiological link with implications for pathogenesis of cardiovascular disease. Circulation 1996;93:1331–3.
[5] Moncada S, Palmer RM, Higgs EA. The discovery of nitric oxide as the endogenous nitrovasodilator. Hypertension 1988;12:365–72.
[6] Steinberg HO, Baron AD. Vascular function, insulin resistance and fatty acids. Diabetologia 2002;45:623–34.
[7] Stuehr DJ. Structure-function aspects in the nitric oxide synthases. Annu Rev Pharmacol Toxicol 1997;37:339–59.
[8] Gratton JP, Fontana J, O'Connor DS, Garcia-Cardena G, McCabe TJ, Sessa WC. Reconstitution of an endothelial nitric-oxide synthase (eNOS), hsp90, and caveolin-1 complex in vitro Evidence that hsp90 facilitates calmodulin stimulated displacement of eNOS from caveolin-1. J Biol Chem 2000;275:22268–72.
[9] Montagnani M, Chen H, Barr VA, Quon MJ. Insulin-stimulated activation of eNOS is independent of Ca^{2+} but requires phosphorylation by Akt at Ser(1179). J Biol Chem 2001;276:30392–8.

[10] Fleming I, Bauersachs J, Fisslthaler B, Busse R. Ca^{2+}-independent activation of the endothelial nitric oxide synthase in response to tyrosine phosphatase inhibitors and fluid shear stress. Circ Res 1998;82:686–95.
[11] Caulin-Glaser T, Garcia-Cardena G, Sarrel P, Sessa WC, Bender JR. 17 beta-estradiol regulation of human endothelial cell basal nitric oxide release, independent of cytosolic Ca^{2+} mobilization. Circ Res 1997;81:885–92.
[12] Tsukahara H, Gordienko DV, Tonshoff B, Gelato MC, Goligorsky MS. Direct demonstration of insulin-like growth factor-I-induced nitric oxide production by endothelial cells. Kidney Int 1994;45:598–604.
[13] Fulton D, Gratton JP, McCabe TJ, Fontana J, Fujio Y, Walsh K, et al. Regulation of endothelium-derived nitric oxide production by the protein kinase Akt. Nature 1999;399:597–601.
[14] Dimmeler S, Fleming I, Fisslthaler B, Hermann C, Busse R, Zeiher AM. Activation of nitric oxide synthase in endothelial cells by Akt-dependent phosphorylation. Nature 1999;399:601–5.
[15] Saltiel AR, Kahn CR. Insulin signalling and the regulation of glucose and lipid metabolism. Nature 2001;414:799–806.
[16] Flatt PR, Bailey CJ. Abnormal plasma glucose and insulin responses in heterozygous lean (ob/+) mice. Diabetologia 1981;20:573–7.
[17] Palmer AM, Thomas CR, Gopaul N, Dhir S, Anggard EE, Poston L, et al. Dietary antioxidant supplementation reduces lipid peroxidation but impairs vascular function in small mesenteric arteries of the streptozotocin-diabetic rat. Diabetologia 1998;41:148–56.
[18] Kojima H, Sakurai K, Kikuchi K, Kawahara S, Kirino Y, Nagoshi H, et al. Development of a fluorescent indicator for nitric oxide based on the fluorescein chromophore. Chem Pharm Bull 1998;46:373–5.
[19] Kojima H, Urano Y, Kikuchi K, Higuchi T, Hirata Y, Nagano T. Fluorescent indicators for imaging nitric oxide production. Angew Chem Int Ed Engl 1999;38:3209–12.
[20] Grynkiewicz G, Poenie M, Tsien RY. A new generation of Ca^{2+} indicators with greatly improved fluorescence properties. J Biol Chem 1985;260:3440–50.
[21] Blute TA, Lee MR, Eldred WD. Direct imaging of NMDA-stimulated nitric oxide production in the retina. Vis Neurosci 2000;17:557–66.
[22] Broillet M, Randin O, Chatton J. Photoactivation and calcium sensitivity of the fluorescent NO indicator 45-diaminofluorescein (DAF-2): implications for cellular NO imaging. FEBS Lett 2001;491:227–32.
[23] Zhang X, Kim WS, Hatcher N, Potgieter K, Moroz LL, Gillette R, et al. Interfering with nitric oxide measurements. 4,5-Diaminofluorescein reacts with dehydroascorbic acid and ascorbic acid. J Biol Chem 2002;277:48472–8.
[24] Suzuki N, Kojima H, Urano Y, Kikuchi K, Hirata Y, Nagano T. Orthogonality of calcium concentration and ability of 4,5-diaminofluorescein to detect NO. J Biol Chem 2002;277:47–9.
[25] Takumida M, Anniko M. Simultaneous detection of both nitric oxide and reactive oxygen species in guinea pig vestibular sensory cells. ORL J Otorhinolaryngol Relat Spec 2002;64:143–7.
[26] Smith PK, Krohn RI, Hermanson GT, Mallia AK, Gartner FH, Provenzano MD, et al. Measurement of protein using bicinchoninic acid. Anal Biochem 1985;150:76–85.
[27] Misko TP, Schilling RJ, Salvemini D, Moore WM, Currie MG. A fluorometric assay for the measurement of nitrite in biological samples. Anal Biochem 1993;214:11–6.
[28] Tran QK, Ohashi K, Watanabe H. Calcium signalling in endothelial cells. Cardiovasc Res 2000;48:13–22.
[29] Kojima H, Nakatsubo N, Kikuchi K, Urano Y, Higuchi T, Tanaka J, Kudo Y, Nagano T. Direct evidence of NO production in rat hippocampus and cortex using a new fluorescent indicator: DAF-2 DA. NeuroReport 1998;9:3345–8.
[30] Zeng G, Quon MJ. Insulin-stimulated production of nitric oxide is inhibited by wortmannin direct measurement in vascular endothelial cells. J Clin Invest 1996;98:894–8.
[31] Arcaro A, Wymann MP. Wortmannin is a potent phosphatidylinositol 3-kinase inhibitor: the role of phosphatidylinositol 3,4,5-trisphosphate in neutrophil responses. Biochem J 1993;296(Pt 2):297–301.
[32] Hu Y, Qiao L, Wang S, Rong SB, Meuillet EJ, Berggren M, et al. 3-(Hydroxymethyl)-bearing phosphatidylinositol ether lipid analogues and carbonate surrogates block PI3-K, Akt, and cancer cell growth. J Med Chem 2000;43:3045–51.
[33] Montagnani M, Quon MJ. Insulin action in vascular endothelium: potential mechanisms linking insulin resistance with hypertension. Diabetes Obes Metab 2000;2:285–92.
[34] Zeng G, Nystrom FH, Ravichandran LV, Cong LN, Kirby M, Mostowski H, et al. Roles for insulin receptor, PI3-kinase, and Akt in insulin-signaling pathways related to production of nitric oxide in human vascular endothelial cells. Circulation 2000;101:1539–45.
[35] Fisslthaler B, Benzing T, Busse R, Fleming I. Insulin enhances the expression of the endothelial nitric oxide synthase in native endothelial cells: a dual role for Akt and AP-1. Nitric Oxide 2003; 8:253–61.
[36] Federici M, Pandolfi A, De Filippis EA, Pellegrini G, Menghini R, Lauro D, et al. G972R IRS-1 variant impairs insulin regulation of endothelial nitric oxide synthase in cultured human endothelial cells. Circulation 2004;109:399–405.
[37] Isenovic ER, Divald A, Milivojevic N, Grgurevic T, Fisher SE, Sowers JR. Interactive effects of insulin-like growth factor-1 and beta-estradiol on endothelial nitric oxide synthase activity in rat aortic endothelial cells. Metabolism 2003;52:482–7.
[38] Yki-Jarvinen H, Utriainen T. Insulin-induced vasodilatation: physiology or pharmacology? Diabetologia 1998;41:369–79.
[39] Zierath JR, Krook A, Wallberg-Henriksson H. Insulin action and insulin resistance in human skeletal muscle. Diabetologia 2000;43: 821–35.
[40] Jiang ZY, Lin YW, Clemont A, Feener EP, Hein KD, Igarashi M, et al. Characterization of selective resistance to insulin signaling in the vasculature of obese Zucker (fa/fa) rats. J Clin Invest 1999;104:447–57.
[41] Vicent D, Ilany J, Kondo T, Naruse K, Fisher SJ, Kisanuki YY, et al. The role of endothelial insulin signaling in the regulation of vascular tone and insulin resistance. J Clin Invest 2003;111: 1373–80.
[42] Vehkavaara S, Makimattila S, Schlenzka A, Vakkilainen J, Westerbacka J, Yki-Jarvinen H. Insulin therapy improves endothelial function in type 2 diabetes. Arterioscler Thromb Vasc Biol 2000;20:545–50.
[43] Pieper GM. Review of alterations in endothelial nitric oxide production in diabetes: protective role of arginine on endothelial dysfunction. Hypertension 1998;31:1047–60.